
Visualization of Damaged Brain Tissue After Ischemic Stroke with Cobalt-55 Positron Emission Tomography

H.M.L. Jansen, J. Pruijm, A.M. v.d. Vliet, A.M.J. Paans, J.M. Hew, E.J.F. Franssen, B.M. de Jong, J.G.W. Kosterink, R. Haaxma and J. Korf

Departments of Biological Psychiatry, Neurology, PET-Research Center, and Departments of Neuro-Radiology and Pharmacy, University Hospital Groningen, The Netherlands

In animal experiments, the radionuclide $^{55}\text{Co}^{2+}$ has been shown to accumulate in degenerating cerebral tissue similar to Ca^{2+} . **Methods:** The potential role of $^{55}\text{Co}^{2+}$ for in vivo brain PET imaging was investigated in four patients after ischemic stroke. **Results:** PET showed uptake of $^{55}\text{Co}^{2+}$ in damaged brain tissue irrespective of blood-brain barrier integrity, as affirmed by CT and MRI. **Conclusion:** Our preliminary results indicate that $^{55}\text{CoCl}_2$ may prove to be a useful and relatively inexpensive PET radiopharmaceutical for visualization of degenerative processes in brain tissue.

Key Words: cobalt; PET; ischemic damage; stroke

J Nucl Med 1994; 35:456-460

Brain imaging techniques used for detection of morphological changes in stroke (CT, MRI) permit demonstration of infarcts, perifocal edema and disruption of blood-brain barrier (BBB) integrity, but pathophysiologic alterations leading to reversible or irreversible ischemic brain damage cannot be visualized. With PET, regional cerebral blood-flow (rCBF) and brain metabolism were studied extensively (1,2). However, despite a considerable increase in our understanding of the pathophysiology of stroke using PET, determining the degree of neurological residual deficit and prediction of clinical outcome in cerebrovascular accidents (CVA) still remains a problem.

We propose the use of cobalt as a calcium indicator to visualize ischemic brain damage in the early phase of stroke. The principle of our approach is based on the well documented fact that calcium (Ca) accumulates in degenerating (nerve) tissue (3). Elevation in intracellular calcium is closely linked with the process of cell death following ischemic injury (4). Thus, autoradiography of ^{45}Ca of brain sections of cats and rats exposed to ischemia allow the

visualization of damaged brain tissue independent of BBB integrity (5-8). Since there is no calcium isotope with suitable radiation characteristics for PET, we suggest ^{55}Co as a neuronal calcium marker and indicator of endangered brain tissue (9). The usefulness of cobalt to trace calcium has already been established since cobalt ions accumulate in ischemia damaged brain tissue both in vitro and in vivo (5-7,9-12).

In several experiments cobalt uptake was identified histochemically and correlated with calcium accumulation through divalent cation-permeable kainate-activated receptor-operated channels (5-7,12). A detectable uptake of cobalt was visualized by cobalt-sulfide histochemistry in experiments in which calcium influx was stimulated by excitatory amino acids (EAA) (6). Moreover, silverstaining showed selective neuronal cobalt uptake following kainate application with or without the presence of a selective kainate receptor antagonist (7). In addition, cobalt entry in fura-2-loaded neurons was monitored using fura-2-based microfluorimetry with cobalt as the extracellular divalent cation which quenches emitted fluorescence from fura-2 (7,12). These results are in agreement with previous observations using ^{45}Ca autoradiography in which ^{55}Co can be applied as a marker for calcium uptake in animal brain (5). Cobalt-55 is a convenient radionuclide for PET due to its physical properties ($T_{1/2}$ 17.5 hr, 77% β^+ , $E_{\beta^+\text{max}}$ = 1.513 MeV, two main energies at 477 keV (20.3%) and 931 keV (75%) and emission of gamma-quanta at other energies) and pharmacological properties (rapid renal clearance and fecal excretion after intravenous administration, although a small fraction of the administered dose has a biological half-life of about 2 yr) (13,14).

It is expected that the administration of ^{55}Co and subsequent PET may enable the detection of very recent ischemic lesions, yielding additional information that cannot be provided by CT, MRI or MRS. Consequently, ^{55}Co may prove to be a sensitive and early marker for cell death that enables early diagnosis of stroke and permits estimation of the extent of cerebral tissue at risk. In this way, assessing the efficacy of (experimental) therapeutic interventions to reduce brain ischemic damage may become possible.

Received Aug. 30, 1993; revision accepted Dec. 14, 1993.

For correspondence and reprints contact: H.M.L. Jansen, Depts. of Biological Psychiatry and Neurology, University Hospital Groningen, P.O. Box 30.001, 9700 RB Groningen, The Netherlands.

MATERIALS AND METHODS

The patients were examined by cranial CT. The first examination took place before and after administration of intravenous contrast. The second examination was performed after 3 hr. MRI scans were also obtained, both with and without contrast medium (Gadolinium-DTPA). Hereafter, patients received $^{55}\text{CoCl}_2$ intravenously 24 ± 6 hr before PET imaging and at least 6 hr after administration of gadolinium-DTPA.

Cobalt-55 was produced by the ^{56}Fe (p, 2n) ^{55}Co nuclear reaction using a 27-MeV proton beam from the AVF-cyclotron of the Technical University in Eindhoven (The Netherlands). The yield is 67 MBq/ μAh (1.8 mCi/ μAh). After irradiation, the iron target (0.5 mm thick) was dissolved in a mixture of sulfuric acid and nitric acid. After extraction of the bulk of the Fe, a final Fe-Co separation is accomplished on a Dowex anion exchange column according to the prescription of Lagunas-Solar (15). Radionuclide impurities are ^{56}Co , ^{57}Co and ^{52}Mn . Radiochemical purity was verified by thin-layer chromatography and absence of organic solvents was established by gas chromatography.

Quantification of ^{56}Co ($T_{1/2}$ 78,8 days, 19% β^+ , $E_{\beta^+ \text{max}}$ = 1,459 MeV, numerous high energy gamma lines between 850 keV and 3 MeV) contamination was performed by gamma ray spectroscopy (13). The use of ^{55}Co is limited up to about 48 hr after irradiation due to ^{56}Co contaminant. At that moment a maximum of 5% ^{56}Co will be present. The amount of ^{56}Co in the final product has to be limited because of its radiation characteristics and its half-life of 78.8 days. The presence of ^{56}Co cannot be avoided due to nuclear properties involved in the production process (15–17). Based on animal data, the radiation dose of $^{55}\text{CoCl}_2$ and $^{56}\text{CoCl}_2$ were calculated to be 0.062 mSv/MBq (0.23 rad/mCi) and 1.28 mSv/MBq (4.75 rad/mCi), respectively (15–17). An overall retention time was obtained from the animal data. Assuming a uniform distribution, a first-order approximation of the total body dose was calculated based on the energy release per disintegration. A more accurate total body dose will be calculated based on the actual distribution as a function of time as measured by whole-body scanning in future studies. With a limited total radiation dose of 5 mSv (in accordance with the guidelines of our Medical Ethics Committee), the amount of ^{56}Co had to be limited to 5.7% at the moment of injection. Cobalt-57 contamination is minor and only measurable after decay of ^{55}Co .

The four patients (3 men, 1 woman) had to meet the following criteria: 50 yr of age or older, neurologic symptomatology in agreement with an acute cortical ischemic stroke, clear consciousness and admission between 24 hr and 72 hr after onset of the accident. Patients presenting any of the following were excluded: pregnancy, history of allergy, claustrophobia, pacemaker in situ and clipped aneurysm in cerebro. All patients gave a written informed consent. The study was conducted in accordance with guidelines from the Medical Ethics Committee of the University Hospital.

Imaging was performed after injection (1–2 mCi sterile $^{55}\text{CoCl}_2$, Cygne BV, Eindhoven, The Netherlands) using a Siemens ECAT-951/31 positron camera consisting of two rings of BGO block-detectors with a total axial length of 10.8 cm, divided into 31 transaxial images, 16 straight-planes and 15 cross-planes. The spatial resolution of the camera in stationary mode is 6 mm FWHM. Since the energy window is set from 250 to 850 keV, it is not possible to discard the 477 keV gamma ray of ^{55}Co (abundance 20.3%). Scans were made parallel to the orbitomeatal line and reconstructed to 6-mm thick planes using standard ECAT-

software. The infarcted region in the brain was outlined as a region of interest (ROI) and the average amount of activity in the ROI was measured. In order to determine the ratio infarcted-to-noninfarcted (background) uptake in the brain, the average uptake in a nonaffected part of the brain was determined.

CT was performed before and after administration of 100 ml of a nonionic contrast medium (Omnipaque; 300 mg I/ml) intravenously. A repeated plain scan was made 3 hr after the last (contrast) scan to evaluate the integrity of the BBB. All the examinations took place on a Philips Tomoscan 310. Contiguous 6-mm thick slices were made parallel to the orbitomeatal line.

MRI was performed on a Philips Gyroscan S15 with a 1.5 T superconducting magnet. Transverse 6-mm-thick slices with a 10% gap were made parallel to the orbitomeatal line. Both T_1 (TR/TE 700/20) and T_2 (TR/TE 2000/50-110) images were made, followed by enhanced T_1 (TR/TE 700/20) images after administering 0.1 mmole/kg Gadolinium-DTPA (Magnevist, Schering) intravenously. The total MRI scan time did not exceed 30 min.

RESULTS

Four patients were included in our study. In all patients, clear uptake of ^{55}Co was demonstrated in the affected hemisphere.

Patient One

A 68-yr-old female presented with acute onset of nausea, vomiting and mild central paresis on the right side of the body, including facial musculature. CT revealed periventricular white matter lesions and slight widening of the insular sulci, probably due to previous infarction. Postcontrast CT showed no pathological enhancement. Repeated plain CT revealed no changes. Bright periventricular lesions were noted on the T2-weighted MR images. On the T1-weighted images, some of the nonspecified white matter lesions were hypointense. The insular sulci were slightly widened. Postgadolinium-DTPA showed no enhancement.

PET imaging was performed 48 hr after occurrence of the first symptoms and 25 hr after administration of 2 mCi ^{55}Co . In both the right and left parietal regions of the brain, relative accumulation of ^{55}Co was seen. The diameter of the left parietal lesion was 15 mm. Activity in that region was 3.4 times that of the background activity in the brain.

Patient Two

A left-handed 52-yr-old male presented with acute onset of mixed aphasia and mild left-sided weakness, especially clumsiness of the left arm (Fig. 1).

On plain CT, there was a poorly demarcated hypodense lesion in the right temporo-parietal region. Postcontrast CT showed no enhancement. Repeated plain CT revealed no changes.

The lesion was hyperintense on the T2-weighted MR images and hypointense on the T1-weighted images. Postgadolinium-DTPA imaging showed vascular enhancement of the cortical region and no signs of BBB disruption.

PET scanning, performed 60 hr after occurrence of the first symptoms and 18 hr after administration of 2 mCi of

^{55}Co , showed accumulation in an area 55×23 mm. Activity was five times the background activity of the brain.

Patient Three

A 79-yr-old male was admitted to the hospital with complete stroke presenting as left-sided hypertonic hemiparesis with brisk tendon reflexes and Babinski sign left, hemi-inattention and hemi-anopia left (Fig. 2).

On MRI, two lesions in the right parietal and occipital region were seen, both hyperintense on the T2-weighted images and hypointense on the native T1-weighted images. Postgadolinium-DTPA showed intraparenchymal contrast leakage in both regions, indicating BBB disruption.

PET scanning, performed 80 hr after completion of the stroke and 20 hr after administration of 2 mCi of ^{55}Co , showed accumulation of ^{55}Co in both parietal and occipital affected regions of the brain. Activity in both regions was 2.9 times the background activity of the brain. The diameter of the left parietal lesion was 50×30 mm; the left occipital region was 52×24 mm.

Patient Four

A 60-yr-old male presented with progressive stroke, showing mixed aphasia and mild right-sided weakness.

On MRI, a lesion was seen in the left temporal region. It was hyperintense on the T2-weighted image and hypointense on the native T1-weighted image. Postgadolinium-DTPA showed no enhancement.

PET scanning, performed 20 hr after onset of the first symptoms and 8 hr after administration of 1 mCi of ^{55}Co , showed accumulation of ^{55}Co in the left temporal region. Activity in this region was 1.3 times the background activity of the brain. The diameter of the lesion was 35×45 mm.

DISCUSSION

In four stroke patients, we visualized brain damage using PET by detection of regionally specific accumulation of ^{55}Co . Three of these patients had an intact BBB (as affirmed by CT or MRI); one of the patients clearly had a compromised BBB with intraparenchymal contrast leakage.

The basic mechanism of detection in ^{55}Co PET is extravasation of intravenous ^{55}Co into the affected brain areas irrespective of BBB integrity. In the case of hemorrhage, ^{55}Co will intensely stain the hemorrhagic site due to ^{55}Co contained in the blood. In the event of BBB disruption, ^{55}Co will leak passively through a compromised BBB. In the case of BBB integrity, ^{55}Co is supposed to cross the BBB and to accumulate specifically in endangered brain tissue. However, extravasation of ^{55}Co can be prevented by absence of perfusion due to collapsed microcirculation as a result of extensive early (cytotoxic) and/or late (vasogenic) edema. In fact, fluid accumulation from early edema may explain the sensitivity of T2-weighted and diffusion-MRI to early infarction when BBB breakdown and late edema are absent.

In Patient 1, MRI and CT showed no evidence of the

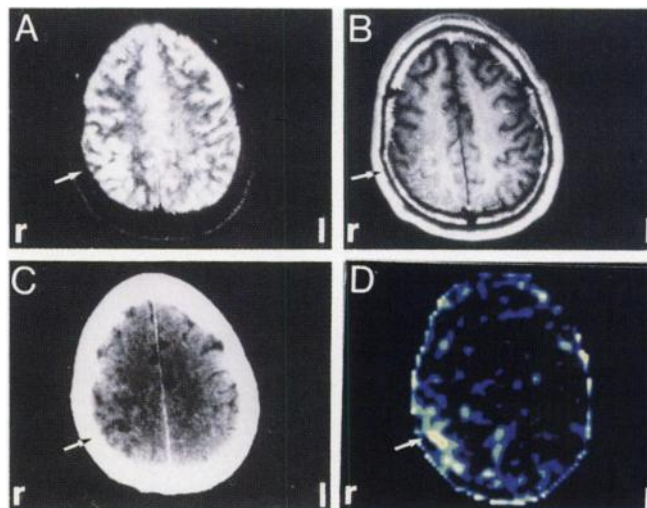


FIGURE 1. T2-weighted (A) and postgadolinium-DTPA T1-weighted (B) MR images of Patient 2 show a hyperintense lesion (A) in the right parietal region with vascular enhancement (B) and no sign of BBB disruption (B). Postcontrast CT (C) exhibits a poorly demarcated hypodense lesion in the right parietal region without signs of BBB disruption. Cobalt-55 image-PET (D) demonstrates evident uptake (five times the background activity) in the region of interest. Activity in the skull was masked.

(clinically) suspected infarction in the left cerebral hemisphere. PET showed uptake of ^{55}Co in both right and left parietal lobe. The uptake in the left parietal region is compatible with the affected part of the brain that gave rise to the aforementioned paralysis. The additional uptake contralateral to the clinically appropriate ^{55}Co accumulation, suggests a clinically silent infarction illustrating the high sensitivity of ^{55}Co PET for early damage. Involvement of both hemispheres is not unusual in a decreased posterior cerebral circulation.

In Patient 2, the lesion was predominantly visible on MRI on the T2-weighted images, suggesting tissue decay (Fig. 1). Nevertheless, on the postgadolinium-DTPA scan, there was no evidence of BBB disruption. The cortical vessels showed some vascular enhancement possibly due to luxury perfusion. Postcontrast CT findings (no enhancement) affirmed the BBB integrity. PET showed clear uptake of ^{55}Co in the right temporo-parietal region. Its appearance and convexity in the midline area are not concomitant with BBB disruption and/or hemorrhage on CT or MRI. These additional sites may not be due to tissue damage but rather to focal accumulation of ^{55}Co in (venous) blood.

In Patient 3, MRI clearly showed two separate subacute infarctions in the right hemisphere, both on the T2-weighted images and on the postgadolinium-DTPA T1-weighted images (Fig. 2). Contrast-enhancement on the postgadolinium T1-weighted images is due to contrast-leakage through a disrupted BBB. There were no signs of hemorrhage as could be seen on the pre-gadolinium T1-weighted images (absence of high signals). PET showed clear uptake of ^{55}Co in both the right parietal and occipital

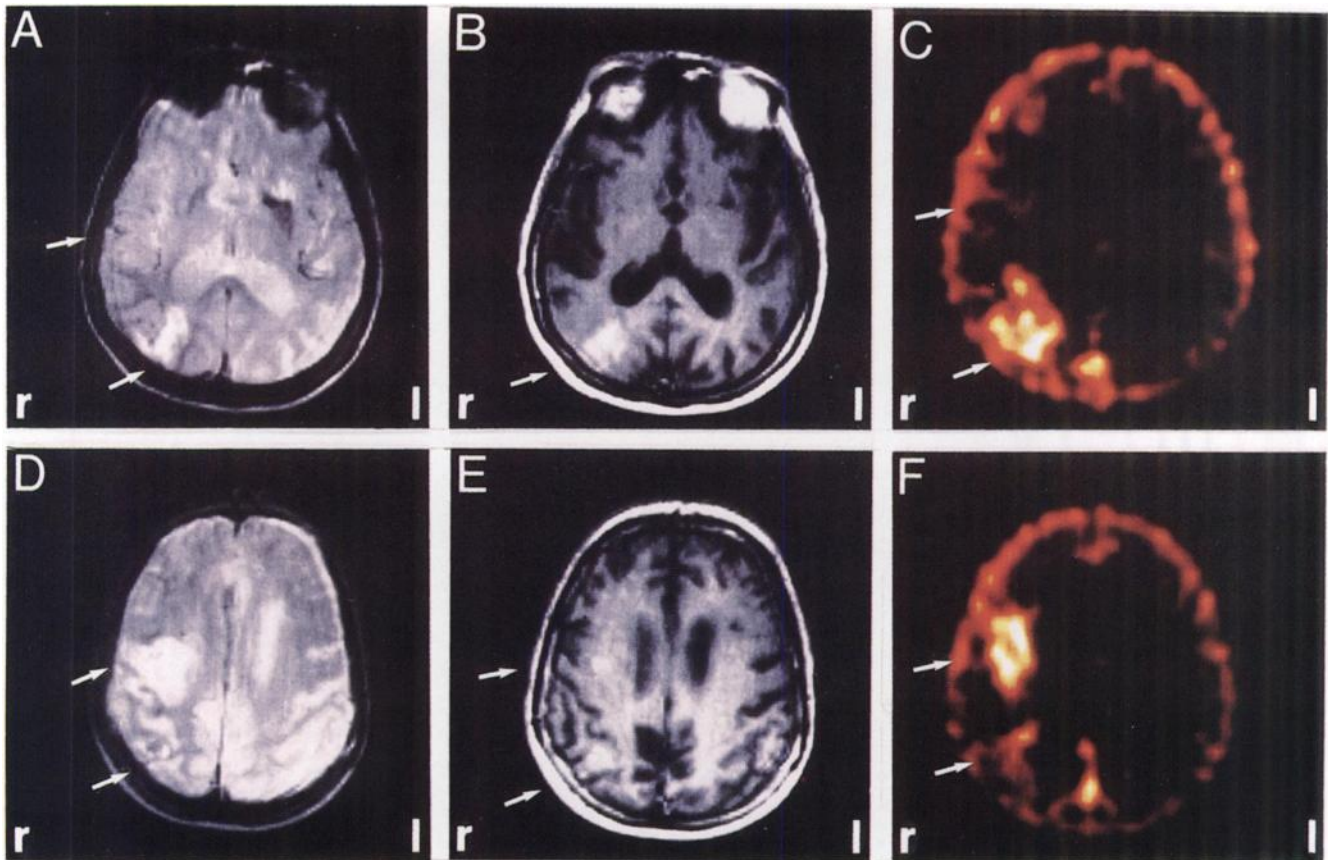


FIGURE 2. T2-weighted (A,D), postgadolinium-DTPA T1-weighted (B,E) and ^{55}Co PET (C,F) images of Patient 3 demonstrate two infarctions with signs of BBB disruption (intraparenchymal contrast leakage on B,E) and edema (hyperintensity on A,D) in the right parietal and occipital regions. Cobalt-55 PET image shows evident uptake (2.9 times the background activity) in both regions of interest. Activity in the skull was masked.

sites. The ^{55}Co appearance in the midline area and convexity is once again supposed to be due to radiotracer contained in venous blood. There is a striking similarity in ^{55}Co uptake in both infarcted sites, possibly reflecting a similar uptake mechanism (passive accumulation through a compromised BBB).

In Patient 4, the left temporal lesion was visible both on the T2-weighted and T1-weighted MR images. There were no signs of BBB disruption. In the left temporal region there was moderate ^{55}Co uptake, although it was highly regional specific. This moderate ^{55}Co uptake may possibly be due to the relatively short period (8 hr) between administration of ^{55}Co and PET acquisition, selective ^{55}Co -transport across an intact BBB and a relatively low dose of ^{55}Co (1 mCi).

In stroke patients, the following aspects may contribute to lesion detectability by ^{55}Co PET: extent and duration of ischemia; permeability of the BBB; the postinfarct period; ^{55}Co dose; plasma-protein binding of ^{55}Co ; the time interval between administration of ^{55}Co and PET acquisition; and scanner resolution.

The extent of ischemia is the main factor determining infarction size. BBB permeability depends on the time after onset of stroke and the duration of ischemia. The amount of ^{55}Co available for BBB transfer is determined by

the administered dose of ^{55}Co , the amount and nature of the ^{55}Co plasma-protein binding and the time interval between administration of ^{55}Co and PET acquisition. Cobalt-55 is supposed to transfer an intact BBB in three possible manners: free unbound $^{55}\text{Co}^{2+}$ -ions, reversible plasma-protein bound ^{55}Co after dissociation at the ischemic site and ^{55}Co bound to very small plasma-proteins able to cross the BBB as an organo-metal complex. The PET scanner's resolution evidently depends on the physical design of the device and the achievable signal-to-noise ratio. The distribution of systematically administered ^{55}Co in the brain is, apart from ^{55}Co contained in venous blood, specific to ischemic lesions, since unaffected nonischemic brain tissue and cerebrospinal fluid (CSF) shows very low ^{55}Co uptake, indicating intact efficient BBB function for ^{55}Co .

Whether or not ^{55}Co accumulates in ischemic brain lesions *in vivo* in a way similar to *in vitro* neuronal uptake (^{55}Co as a calcium marker entering the cell through calcium-permeable KA-activated channels in the neuronal membrane) is a question requiring further investigation (9,18-21).

So far we have successfully studied four patients. We are, however, aware of both the potential of this approach and the preliminary nature of our data, which purport ^{55}Co

to be a possible marker for ischemic injury. Additional data on ^{55}Co PET are necessary before reaching a more definitive answer whether ^{55}Co PET may become a tool in estimating brain pathology quantitatively in CVA as well as in other degenerative diseases. Because calcium influx is also increased in areas affected by secondary degenerative processes, visualization of such brain areas, showing antero cq retrograde degeneration as a result of the primary infarction, may become possible.

ACKNOWLEDGMENT

The authors thank Cygne BV for providing $^{55}\text{CoCl}_2$, and Ms. W. van der Meer for excellent secretarial assistance. This work was supported by a grant from the Dutch Technology Foundation (STW).

REFERENCES

1. Phelps ME, Huang SC, Hoffman EJ, Selin C, Sokoloff L, Kuhl DE. Tomographic measurement of local cerebral glucose metabolic rate in humans with (^{18}F) 2-fluoro-2-deoxy-D-glucose: validation of method. *Ann Neurol* 1979;6:371-388.
2. Ter-Pogossian MM, Herscovitch P. Radioactive oxygen-15 in the study of cerebral blood flow, blood volume and oxygen metabolism. *Semin Nucl Med* 1985;25:377-394.
3. Siesjö BK, Bengtsson F. Calcium fluxes, calcium antagonists and calcium related pathology in brain ischemia, hypoglycemia and spreading depression: a unifying hypothesis. *J Cereb Blood Flow Metab* 1989;9:127-140.
4. Dubinsky JM. Examination of the role of calcium in neuronal death. *Ann NY Acad Sci* 1993;679:34-40.
5. Gramsbergen JBP, Veenma-van der Duin L, Loopuijt L, Paans AMJ, Vaalburg W, Korf J. Imaging of the degeneration of neurons and their processes in rat or cat brain by $^{45}\text{CaCl}_2$ autoradiography or $^{55}\text{CoCl}_2$ positron emission tomography. *J Neurochem* 1988;50:1798-1807.
6. Williams LR, Pregonzer JF, Oostveen JA. Induction of cobalt accumulation by excitatory amino acids within neurons of the hippocampal slice. *Brain Res* 1992;581:181-189.
7. Gibbons SJ, Brorson JR, Bleakman D, Chard PS, Miller RJ. Calcium influx and neurodegeneration. *Ann NY Acad Sci* 1993;679:22-33.
8. Dienel GA, Pulsinelli WA. Uptake of radiolabeled ions in normal and ischemia-damaged brain. *Ann Neurol* 1986;19:465-472.
9. Jansen HML, Pruijm J, Paans AMJ, et al. Visualization of ischemic brain damage with ^{55}Co positron emission tomography in man. *J Cereb Blood Flow Metab* 1993;13(suppl 1):S707-708.
10. Llinas RR. The intrinsic electrophysiological properties of mammalian neurons: insights into central nervous system function. *Science* 1988;242:1654-1664.
11. Ascher P, Nowak L. Electrophysiological studies of NMDA receptors. *TINS* 1987;10:284-288.
12. Pruss RM, Akeson RL, Racke MM, Wilburn JL. Agonist-activated cobalt uptake identifies divalent cation-permeable kainate receptors on neurons and glial cells. *Neuron* 1991;7:509-518.
13. Lederer CM, Shirley VS, eds. *Table of isotopes, seventh edition*. New York: Wiley; 1978:158, 162.
14. IARC Working Group on the evaluation of carcinogenic risks to humans. Cobalt and cobalt compounds. Lyon, France: IARC; 1991;52:363-472.
15. Lagunas-Solar MC, Jungerman JA. Cyclotron production of carrier-free cobalt-55, a new positron-emitting label for bleomycin. *Int J Appl Rad Isotopes* 1979;30:25-32.
16. Blottner A, Deckart H, Weiland J. Pharmakokinetik von ^{111}In - und ^{57}Co -Bleomycin. *Radiobiol Radiother* 1978;19:365-377.
17. Paans AMJ, Wiegman T, de Graaf EJ, Kuilman T. *The production and imaging of ^{55}Co -labeled bleomycin*. Gendreau G. Ninth international conference on cyclotrons and their applications. Caen, France: Les Ulis, Les editions de physique; 1981:699-701.
18. Barnes JM, Henley JM. Molecular characteristics of excitatory amino acid receptors. *Prog Neurobiol* 1992;39:113-133.
19. Wood JN, Winter J, James IF, Rang HP, Yeats J, Bevan S. Capsaicin-induced ion fluxes in dorsal root ganglion cells in culture. *J Neurosci* 1988;8:3208-3220.
20. Müller T, Möller T, Berger T, Schnitzer J, Kettenmann H. Calcium entry through kainate receptors and resulting potassium-channel blockade in Bergmann glial cells. *Science* 1992;256:1563-1566.
21. Hollmann M, Hartley M, Heinemann S. Ca^{2+} permeability of KA-AMPA-gated glutamate receptor channels depends on subunit composition. *Science* 1991;252:851-853.